

Measuring the thermal conductivity of the GaN buffer layer in AlGaN/GaN HEMTs: Effect of carbon and iron doping

M.Power^{1,2,*}, J.W. Pomeroy¹, Y.Otoki³, T.Tanaka³, J.Wada³, M. Kuzuhara⁴, W. Jantz⁵, A.Souzis⁶ and M.Kuball¹

¹ Center for Device Thermography and Reliability, H.H. Wills Physics Laboratory, University of Bristol, Tyndall Avenue, Bristol BS8 1TL, UK

² Bristol Centre for Functional Nanomaterials, Centre for Nanoscience and Quantum Information, University of Bristol, Tyndall Avenue, Bristol, BS8 1FD, UK

* Email: maire.power@bristol.ac.uk, Phone: +44 117 928 8750

³ Hitachi Metals, Ltd., Isagozawa 880, Hitachi City, Ibaraki 319-1418, Japan

⁴ Graduate School of Engineering, University of Fukui, 3-9-1 Bunkyo, Fukui 910-8507, Japan

⁵ SemiMap Scientific Instruments GmbH, Tullastr. 67, D79108 Freiburg, Germany

⁶ II-VI Wide Bandgap Group, 20 Chapin Road, Suite 1007, PO Box 840, Pine Brook, NJ 07058, USA

Keywords: Thermal conductivity, GaN, Fe-doping, C-doping, micro-Raman thermography, diamond microparticles.

Abstract

A thermal conductivity of $200 \pm 20 \text{ Wm}^{-1}\text{K}^{-1}$ has been determined for the carbon-doped (concentration of 10^{17} cm^{-3}) GaN buffer layer of an AlGaN/GaN HEMT using new experimental techniques. Micro-Raman thermography combined with diamond micro-thermometry were used to measure the vertical temperature gradient through the device layers and finite element thermal simulation was fit to the measured temperatures to determine the GaN layer thermal conductivity. This technique is beneficial as it can be used on standard device wafers with no additional test structures required. Furthermore we have found that the thermal conductivity of iron-doped (concentration of 10^{18} cm^{-3}) and carbon-doped (concentration of 10^{17} cm^{-3}) buffer layers studied are very similar.

INTRODUCTION

High resistivity GaN buffer layers are indispensable for AlGaN/GaN device performance. The high resistivity buffer realizes good pinch-off stability and high breakdown voltage. However, because the nitrogen vacancy in GaN is a shallow donor, typical undoped GaN is slightly n-type and not highly resistive (typically of the order of $\text{k}\Omega\text{sq}^{-1}$ [1,2]). A variety of techniques have been developed to achieve a high resistivity GaN buffer including carbon (C) doping [3] and iron (Fe) doping [4]. It is important to consider the thermal conductivity of this buffer layer because it has a significant effect on the heat dissipation from the device channel. Furthermore this information is needed for device thermal modelling to estimate the peak channel temperature. Epitaxial undoped GaN layers are generally assumed to have a thermal conductivity of $160 \text{ Wm}^{-1}\text{K}^{-1}$ [5,6]. However, it would be best to confirm these thermal conductivity values through experimental measurement of the vertical temperature gradient through these layers. This can be done using micro-Raman thermography which measures the volumetric depth average and diamond microparticles [7] which measure the surface temperature of such a GaN device layer.

In this work, we determine the vertical temperature gradient within the carbon-doped GaN buffer layer of an AlGaN/GaN ungated HEMT using standard micro-Raman thermography and diamond micro-Raman thermometers. Combining these results with thermal modelling allows us to extract the thermal conductivity of the GaN layer. We also compare devices with carbon and iron-doped GaN buffer layers to quantify any difference in thermal results between the C-doped and Fe-doped buffers.

DEVICE FABRICATION

18 nm AlGaN	18 nm AlGaN	18 nm AlGaN
1.5 μm carbon-doped GaN	0.5 μm undoped GaN	1.2 μm undoped GaN
	1.0 μm carbon-doped GaN	0.3 μm iron-doped GaN
30 nm AlN	30 nm AlN	30 nm AlN
370 μm 6H-SiC (A)	370 μm 6H-SiC (B)	370 μm 6H-SiC (C)

Figure 1: Epilayer structures of devices A, B and C studied.

The epitaxial structures of the devices studied are shown in Figure 1. Semi-insulating 6H-polytype SiC monocrystalline substrates, manufactured by II-VI, were used. These semi-insulating substrates were doped with vanadium with a concentration of approximately $1 \times 10^{17} \text{ cm}^{-3}$. The GaN epitaxial structures were grown by metal organic chemical vapor deposition (MOCVD), using an AIXTRON close-coupled showerhead configuration reactor. Trimethyl-gallium and trimethyl-aluminum were used as group-III atom precursors, and ammonia gas served as the nitrogen precursor. The C-doping in the high resistivity GaN buffer in devices A and B was controlled by utilizing organic residuals from the metalorganic precursors, and controlling incorporation via

MOCVD growth conditions (i.e. flows and substrate temperature). The Fe-doping in the GaN buffer of device C was achieved by modulating the flow rates of bis(cyclopentadienyl)iron (Cp_2Fe) during the GaN growth. The concentrations of carbon and iron were 10^{17} cm^{-3} and 10^{18} cm^{-3} respectively, as measured by secondary ion mass spectroscopy (SIMS). The epi-growth was initialized with the growth of a 30 nm thick AlN nucleation layer on the SiC silicon-surface side, followed by the growth of the high-resistivity carbon-doped GaN buffer or iron-doped GaN buffer. Undoped GaN channels were, then, formed over the high-resistivity buffer layers for devices B and C. Laser interferometers were used to monitor and calibrate the GaN growth rate and thickness. Finally, AlGaN barrier layers with approximately 25 % Al mole fraction and thickness of 18 nm were grown. The AlGaN layers were characterized by measuring the XRD rocking curves with the PANalytical X'PERT MRD system and comparing with simulation. The 2-dimensional electron gas (2DEG) is present underneath the AlGaN barrier. Ungated transistors of 90 μm width were fabricated using Ti/Al/Mo/Au (15/60/35/50 nm) ohmic contacts and 150 nm thick silicon nitride passivation. The devices were mesa isolated with an etching depth of 170 nm using inductively coupled plasma-reactive ion etching (ICP-RIE). The ohmic contacts were separated by 4 μm in the case of device A and by 20 μm in devices B and C.

DEVICE CHARACTERIZATION

Micro-Raman thermography was utilized to measure the volumetric depth average temperature of the GaN layers in ungated transistors A, B and C using the temperature dependence of the GaN $A_1(\text{LO})$ phonon mode. For devices B and C, the temperature extracted was an average through both the undoped GaN layer and the doped GaN buffer. Micro-Raman thermography mapping was performed with a motorized XYZ translation stage having a 0.1 μm step resolution, a 532 nm frequency-doubled Nd:YAG laser (3 mW incident power) and a Renishaw InVia spectrometer. The spot size of the laser on the device surface was 0.5 μm . Lateral maps were recorded from the center of the channel between contacts to 55 μm outside the active device area beyond the mesa edge of the ungated transistors as illustrated in Figure 3A. Device A was DC-biased with a power of 1.24 W and devices B and C were DC-biased with a power of 0.98 W.

A suspension of <1 μm diamond particles in ethanol was spray-deposited over the whole area of device A. This enabled the surface temperature of the device to be determined. Three of the deposited diamond particles were measured, at positions shown in Figure 3. The temperature of the diamond particles was recorded by micro-Raman thermography using the temperature dependence of the diamond 1332 cm^{-1} phonon line. In the DC steady-state measurements performed here, the diamond particle is in thermal equilibrium with the device surface, so the temperature of the diamond particle is the same as the surface temperature of the GaN layer be-

neath. More details on this measurement approach can be found in reference [7].

A three-dimensional (3D) finite element thermal model of one quarter (due to symmetry) of ungated transistor A was constructed in ANSYS [8]. A uniform 2D heat source was placed at the AlGaN/GaN interface, between contacts, to represent the expected approximate uniform Joule heating. Depth-averaged temperatures as well as surface temperatures (vertical temperature gradient) of the GaN buffer layer were simulated and compared with the experimental data. The GaN buffer thermal conductivity, the AlN nucleation layer thermal resistance and the SiC substrate thermal conductivity were adjusted to best fit the measured temperatures.

RESULTS AND DISCUSSION

In order to extract the thermal conductivity of the carbon-doped GaN buffer layer in ungated transistor A from the experimental data, the SiC substrate thermal conductivity had to be firstly fixed in the thermal model. This SiC thermal conductivity was determined by least squares fitting the simulated temperature profile to the experimentally-determined depth-averaged GaN temperature profile. This temperature profile is outside the device active region, and beyond the mesa edge [9] as shown schematically in Figure 2A.

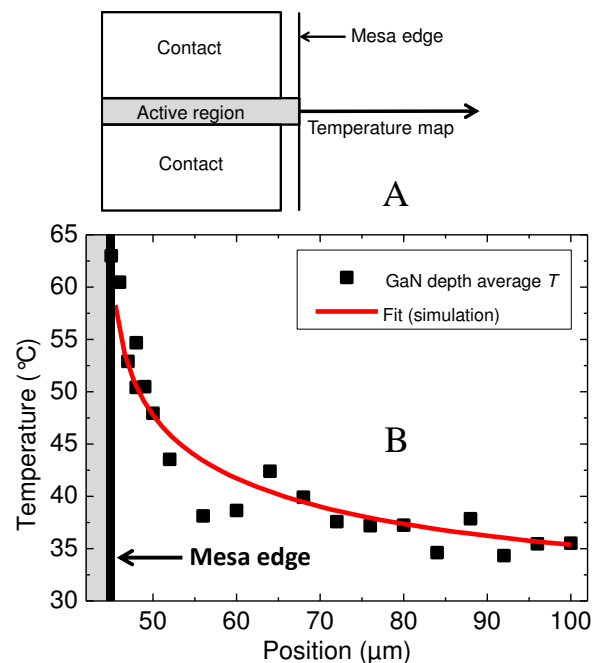


Figure 2: A) Temperature map schematic from mesa edge of ungated transistor A to 55 μm from this edge. B) GaN depth average temperature (T) measured using micro-Raman thermography of the carbon-doped GaN buffer layer in device A and the least squares simulation fit to the data yielding a thermal conductivity of $330 \text{ Wm}^{-1}\text{K}^{-1}$ for the SiC substrate.

This fitting procedure gave a substrate thermal conductivity of $330 \text{ Wm}^{-1}\text{K}^{-1}$ which is in good agreement with literature

values [10] for vanadium-doped SiC. The fit of the thermal simulation to the experimental data is shown in Figure 2B.

Figure 3 shows the surface temperature of and the volumetric depth average temperature through the carbon-doped GaN layer in device A, using diamond microparticles and standard micro-Raman thermography respectively. Least squares fitting of the simulated thermal results to the experimental surface and average GaN layer temperatures gave a thermal conductivity of $200 \text{ Wm}^{-1}\text{K}^{-1}$ for the carbon-doped GaN layer with an estimated range of $\pm 10\%$, represented by the shaded regions. This value matches GaN layer thermal conductivity ranges of $186\text{-}210 \text{ Wm}^{-1}\text{K}^{-1}$ and $185\pm 20 \text{ Wm}^{-1}\text{K}^{-1}$ determined using scanning tunneling microscopy and time domain thermoreflectance found in literature [11] and [12] respectively. The thermal simulation results were found to be insensitive to the thermal boundary resistance parameter associated with the AlN nucleation layer because the temperature gradient through the AlN layer was much smaller than the gradient through the GaN buffer layer for the samples investigated.

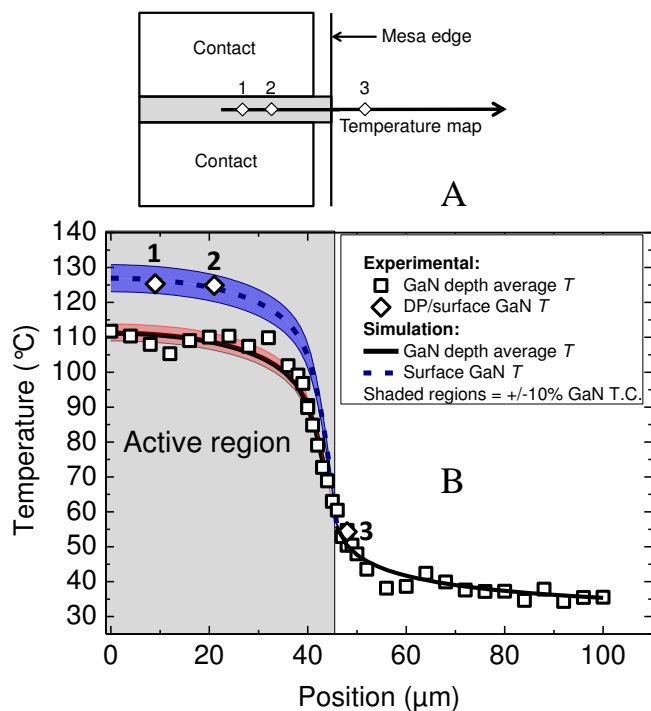


Figure 3: A) Schematic of lateral temperature map from center of ungated transistor A to $55 \mu\text{m}$ beyond the mesa edge B) Depth-averaged temperature determined using micro-Raman thermography and surface temperature extracted using diamond particles (DP) of the carbon-doped GaN buffer layer in device A. Overlaid are the simulated results giving a GaN thermal conductivity (T.C.) of $200 \text{ Wm}^{-1}\text{K}^{-1}$ with shaded regions representing an estimated range of $\pm 10\%$ ($\pm 20 \text{ Wm}^{-1}\text{K}^{-1}$).

Figure 4 shows lateral GaN depth average temperature maps using micro-Raman thermography recorded from the center of ungated transistors B and C to $55 \mu\text{m}$ beyond their mesa edge. It is clear that the temperatures reached in both

devices which have identical dimensions and are biased with the same operating power are very similar within the $\sim 5^\circ\text{C}$ accuracy of the micro-Raman thermography technique. This illustrates that the thermal conductivities of the C-doped and Fe-doped GaN buffer layers in these devices are the same within an accuracy of $\pm 10\%$.

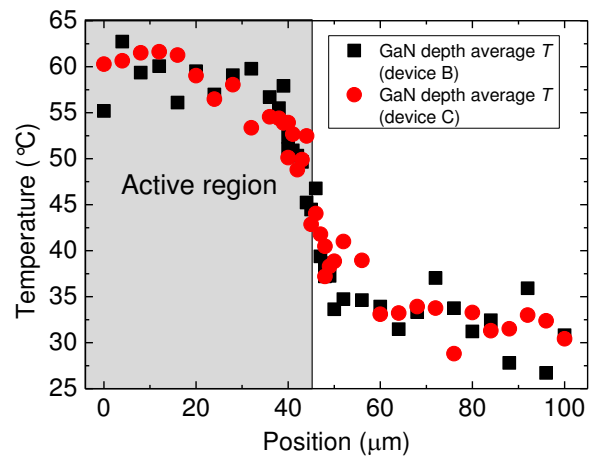


Figure 4: GaN depth-averaged temperature profile using micro-Raman thermography from the center of devices B and C to $55 \mu\text{m}$ beyond their mesa edge.

CONCLUSIONS

A thermal conductivity of $200\pm 20 \text{ Wm}^{-1}\text{K}^{-1}$ was found for the carbon-doped (concentration of 10^{17} cm^{-3}) buffer layer of an AlGaIn/GaN HEMT using a technique comprising micro-Raman thermography, diamond microparticles and finite element thermal simulation. This technique for thermal conductivity measurement is beneficial as a standard device wafer can be used without the need for the fabrication of additional test structures. Furthermore the thermal results of HEMTs with carbon-doped and iron-doped GaN buffer layers were found to be the same within the $\sim 5^\circ\text{C}$ accuracy of the micro-Raman thermography technique indicating an insignificant difference in the thermal conductivity ($< 10\%$) between these doped GaN buffer layers.

ACKNOWLEDGEMENTS

The Engineering and Physical Sciences Research Council (EPSRC), under EP/G036780/1, supported this work. We also acknowledge funding from the EC ENIAC programme, E²coGaN. The authors would like to thank Julián Anaya Calvo and Roland Simon for their guidance.

REFERENCES

- [1] S. Heikman, S. Keller, S. P. DenBaars and U. K. Mishra, Appl. Phys. Lett., **81**, 439 (2002).
- [2] H. Yu, M. K. Ozturk, S. Ozelik and E. Ozbay, J. Cryst. Growth, **293**, 273 (2006).

- [3] J. B. Webb, H. Tang, S. Rolfe and J. A. Bardwell, *Appl. Phys. Lett.*, **75**, 953 (1999).
- [4] M. Rudziński, V. Desmaris, P. A. van Hal, J. L. Weyher, P. R. Hageman, K. Dynefors, T. C. Rödle, H. F. F. Jos, H. Zirath and P. K. Larsen, *Phys. Status Solidi C*, **3**, 2231 (2006).
- [5] L. Yang, S. Ai, Y. Chen, M. Cao, K. Zhang, X. Ma and Y. Hao, *Journal of Semiconductors*, **34**, 074005 (2013).
- [6] M. Kuball, J. M. Hayes, M. J. Uren, T. Martin, J. C. H. Birbeck, R. S. Balmer and B. T. Hughes, *IEEE Electron Device Lett.* **23**, 7 (2002).
- [7] R. B. Simon, J. W. Pomeroy and M. Kuball, *Appl. Phys. Lett.* **104**, 213503 (2014).
- [8] ANSYS®, Academic Research, Release 15.0.
- [9] J. W. Pomeroy, M. Bernardoni, D. C. Dumka, D. M. Fanning and M. Kuball, *Appl. Phys. Lett.* **104**, 083513 (2014).
- [10] S. T. Allen, W. L. Pribble, R. A. Sadler, T. S. Alcorn, Z. Ring and J. W. Palmour, *Microwave Symposium Digest, IEEE MTT-S International*, **1**, 321 (1999).
- [11] D. I. Florescu, V. M. Asnin, F. H. Pollak, A. M. Jones, J. C. Ramer, M. J. Schurman and I. Ferguson, *Appl. Phys. Lett.* **77**, 1464 (2000).
- [12] J. Cho, Y. Li, W. E. Hoke, D. H. Altman, M. Asheghi and K. E. Goodson, *Phys. Rev. B*, **89**, 115301 (2014).

ACRONYMS

AlGaN: Aluminium gallium nitride
 GaN: Gallium nitride
 HEMT: High electron mobility transistor
 SiC: Silicon carbide
 AlN: Aluminium nitride
 XRD: X-ray Diffraction
 MRD: Materials Research Diffractometer
 YAG: Yttrium aluminium garnet
 DC: Direct current
 EC ENIAC: European commission European Nanoelectronics Initiative Advisory Council
 E²coGaN: Energy Efficient Converters using GaN Power Device